

Dynamic NMR and X-ray Studies of Chelated Lithium Phenolates. Tetramers with Pentacoordinate Lithium

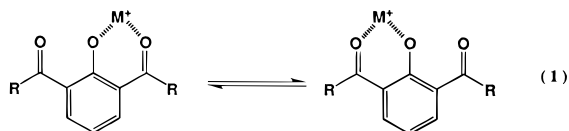
Nikolai A. Khanjin and Fredric M. Menger*

Department of Chemistry, Emory University,
Atlanta, Georgia 30322

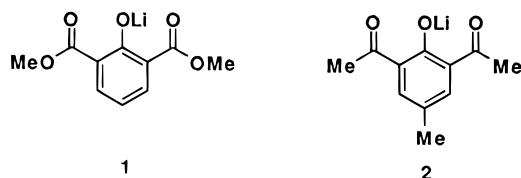
Received June 18, 1997

Introduction

A substantial fraction of synthetically useful reactions are induced by lithium bases. Our particular interest in such compounds centered on lithium phenolates with carbonyl functionalities in both the 2 and 6 positions, thereby enabling the metal to chelate to two oxygens (eq 1, $M^+ = Li^+$). As seen in eq 1, there was also the potential



for the lithium to “oscillate” between the two chelating sites. Such behavior has been observed by dynamic NMR with the corresponding phenols ($M^+ = H^+$).¹ In the course of work involving lithium phenolates **1** and **2**, we



discovered that the lithium is in fact static toward “oscillation” but that, unexpectedly, there are formed two interconvertible and isomeric tetramers which likely contain pentacoordinated lithium. Depending upon solvent, ligands etc., organolithium compounds exist as monomers, dimers, tetramers, and various other aggregates with lithium coordination numbers ranging from 2 to 8.^{2–6} With few exceptions, lithium phenolates form dimeric or tetrameric aggregates having a trigonal or, more commonly, a tetrahedral metal geometry.^{7–9}

Results and Discussion

Reaction of excess LiH with one of the phenols in CD_2Cl_2 , $CDCl_3$, or $THF-d_8$ at ambient temperature afforded

(1) (a) Brzezinski, B.; Denisov, G. S.; Golubev, N. S.; Smirnov, S. N. *J. Mol. Struct.* **1992**, *267*, 383 and references therein; (b) Menger, F. M.; Khanjin, N. A. Unpublished results.

(2) Setzer, W. N.; Schleyer, P. v. R. *Adv. Organomet. Chem.* **1985**, *24*, 353.

(3) Olsher, U.; Izatt, R. M.; Bradshaw, J. S.; Dalley, N. K. *Chem. Rev.* **1991**, *91*, 137.

(4) Gregory, K.; Schleyer, P. v. R.; Snaith, R. *Adv. Inorg. Chem.* **1991**, *37*, 47.

(5) Seebach, D. *Angew. Chem., Int. Ed. Engl.* **1988**, *27*, 1624.

(6) Hilmersson, G.; Davidsson, Ö. *J. Org. Chem.* **1995**, *60*, 7660 and references therein.

(7) For leading references on lithium phenolates, see: Jackman, L. M.; Çizmeçyan, D. *Mag. Reson. Chem.* **1996**, *34*, 14.

(8) (a) Schaaf, P. A.; Jastrzebski, J. T. B. H.; Hogerheide, M. P.; Smeets, W. J. J.; Spek, A. L.; Boersma, J.; van Koten, G. *Inorg. Chem.* **1993**, *32*, 4111; CCDC refcode JUNDEB10 (b) Korobov, M. S.; Minkin, V. I.; Nivorozhkin, L. E.; Kompan, O. E.; Struchkov, Yu. T. *Zh. Obshch. Khim.* **1989**, *59*, 429; CCDC refcode VEGFAO. (c) Harrowfield, J. M.; Skelton, B. W.; White, A. H. *Aust. J. Chem.* **1995**, *48*, 1311; CCDC refcode ZARLAF.

(9) Ball, S. C.; Cragg-Hine, I.; Davidson, M. G.; Davies, R. P.; Lopez-Solera, M. I.; Raithby, P. R.; Reed, D.; Snaith, R.; Vogl, E. M. *J. Chem. Soc., Chem. Commun.* **1995**, 2147; CCDC refcode ZIHCEY.

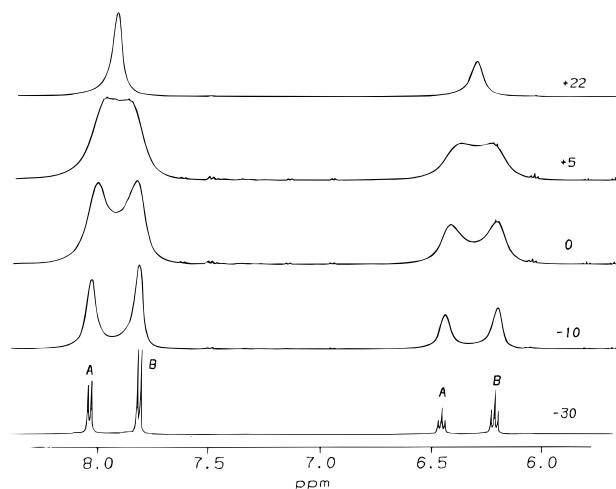


Figure 1. Selected variable temperature 1H NMR spectra (aromatic region) for 0.42 M **I** in CD_2Cl_2 (TMS = 0.0 ppm).

the lithium phenolates **1** and **2**. Pale yellow crystals of **1** were obtained from benzene by slow evaporation at room temperature. Cooling solutions of **2** in warm THF/hexane plus slow evaporation over 2 days also gave yellow crystals. Crystals from both compounds were of X-ray quality, allowing structure determinations as discussed below.

Cryoscopic measurements of **1** in benzene (using a differential scanning calorimeter) gave an average aggregation number of 3.5 ± 0.5 . FAB mass spectrometry showed the presence of $[M]Li^+$, $[M]_2Li^+$, and traces of $[M]_3Li^+$ and $[M]_4Li^+$ ions.

Figure 1 shows 1H NMR spectra (6–8 ppm) of **1** in CD_2Cl_2 as the phenolate was cooled from +22 to -30 °C. It is seen that the *para*-proton at 6.4 ppm transforms from a broad singlet at +22 °C into two sharp triplets (labeled **A** and **B**) at -30 °C. The **A/B** ratio = 3:4. Similarly, the broad singlet at -30 °C of the *meta*-protons (8 ppm) becomes two sharp doublets at -30 °C. Their ratio is likewise 3:4. A broad MeO– singlet (not shown) splits into two sharp singlets at -30 °C with the same **A/B** ratio. No further changes in line shape (e.g. splitting or line broadening) were observed as the sample was cooled down to -90 °C except a decrease in **A/B** ratio to 1:2. Since neither the line shapes nor the ratios of areas change over a 100-fold concentration range (5 mM–0.4 M) at constant temperature, the two exchanging species, **A** and **B**, must be isomeric (i.e. have the same aggregation number) and must interconvert with each other in an intramolecular mechanism. The **A/B** ratio remained constant upon addition of small amounts of THF, TME-DA, or HMPA (up to 3 equiv), but it increased when the entire solvent was changed from CD_2Cl_2 to $CDCl_3$. Thus, the **A/B** ratio = ca. 50 in the latter solvent at -60 °C.

X-ray structures for two different tetramers were obtained from phenolates **1** and **2** (tetramer types **I** and **II**, respectively). Phenolate tetramer of **1** has a distorted D_{2d} symmetry with a typical Li_4O_4 cubical core⁷ (Figure 2).¹² Each lithium therein adopts a square pyramidal configuration in which it is coordinated to three phenolate oxygens in Li_4O_4 core and two *o*-carbonyl oxygens. The complex can be viewed as a “double dimer” in which almost parallel dimer units are offset relative to each other by roughly 90°. Li–O distances within a dimeric unit are ca. 2.0 Å compared with “interdimeric” Li–O bonds (drawn vertically in Figure 2) of ca. 2.2 Å.

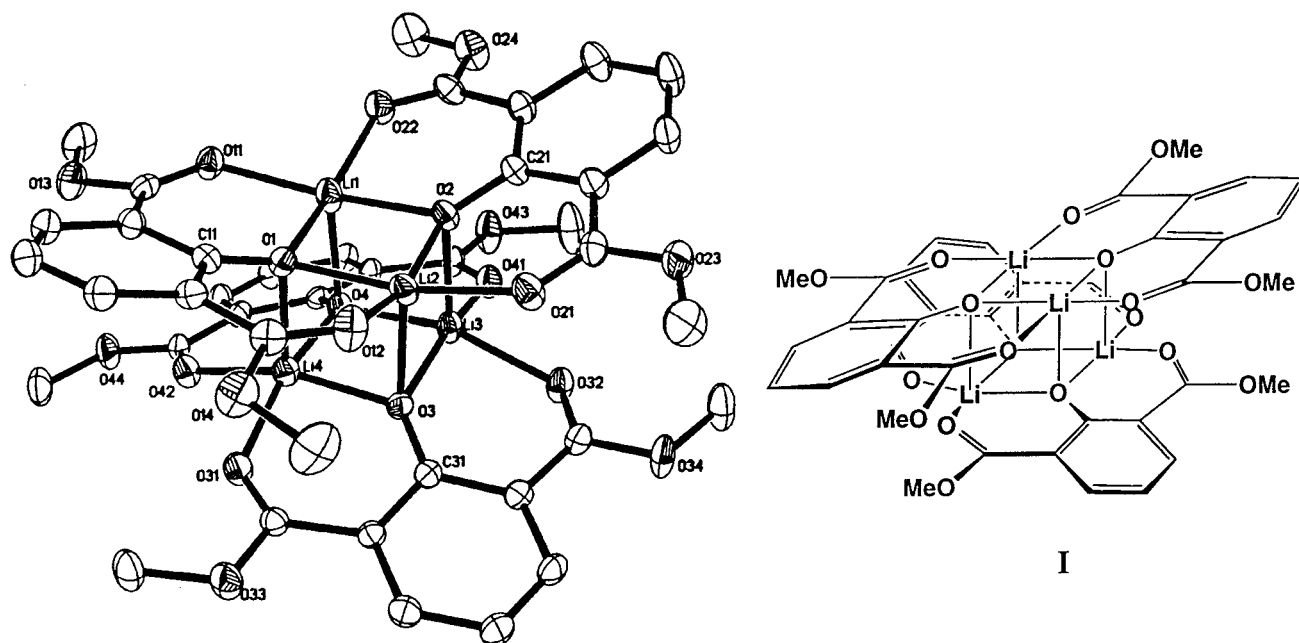


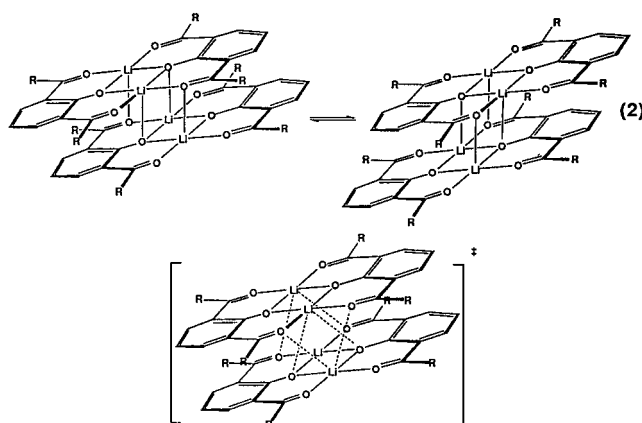
Figure 2. Molecular structure of diester **I** (20% probability thermal ellipsoids). Important bond distances: Li1–O2 2.011 Å, Li1–O22 1.983 Å, Li1–O1 2.001 Å, Li1–O11 2.02 Å, Li1–O4 2.16 Å, Li2–O3 2.193 Å, Li3–O2 2.13 Å, Li4–O1 2.097 Å.

Approximately 30 crystal structures of lithium phenolates have been deposited with the Cambridge Crystallographic Data Centre (CCDC). Of the four X-ray structures reported so far for lithium phenolates with *ortho*-chelating substituents, none forms a tetramer in the solid state. A lithium phenolate with (dimethylamino)methyl substituents at the 2,6-positions is a trimer with a Li_3O_3 planar core and a tetrahedral lithium.^{8a} However, the corresponding sodium phenolate is almost isomorphous with **I**, although interdimeric and intradimeric Na–OAr distances have the same length. The lithium phenolate with *N*-isopropylformimidoyl substituents also has a Li_3O_3 planar core with a tetrahedral lithium.^{8b} The lithium picrate monohydrate crystallizes as a dimer with square pyramidal lithium.^{8c} Finally, *N,N*-ethylenebis(salicylideneiminato)dilithium exists as a dimer in the solid state and resembles **I**; two lithiums in a Li_4O_4 cubical core are pentacoordinated with a distorted trigonal bipyramidal geometry, the other two being tetrahedral and solvated by HMPA.⁹ “Interdimeric” Li–O distances (2.05 Å) are shorter here than “intradimeric” distances (1.98 Å). Thus, to the best of our knowledge, **I** is the first unsolvated Li phenolate with pentacoordinated lithium.

Phenolate **2** is also a “double dimer” in the solid state with C_i point group symmetry, but the two component

sections are now lined up above one another (Figure 3). In this ladder-like structure, the eight acetyl groups and eight *meta*-protons exist in four nonequivalent pairs, whereas the four lithiums and four *para*-protons exist in two non-equivalent pairs. “Vertical” interdimeric Li–O bonds are formed from two equivalent phenolic oxygens and two out of eight carbonyl oxygens (2.11 and 2.35 Å in length, respectively). “Horizontal” intradimeric Li–O distances are only 1.94–2.01 Å.

Consider the possibility that tetramers of type **I** and **II** correspond to **A** and **B** observed in the NMR for phenolate **1**. Although structure **I** has the proper symmetry for the spectra (*i.e.* all aromatic rings are equivalent), this is not true for structure **II**. Thus, if structure **II** happens to be either **A** or **B**, it must engage in an internal reorganization (due to concentration independence of NMR line shapes) that is rapid even at low temperatures. In this reorganization, the two “dimer units” must slide over one another, both frontally and laterally, to render all the aromatic rings equivalent. The former is depicted in eq 2. As shown, the transition state



would involve a symmetric cleavage and reformation of four Li–O bonds as each lithium “jumps” from one oxygen to its immediate equivalent neighbor 3.65 or 3.83 Å away.

(10) In addition to phenolate **1**, we have also examined phenolate **2**, lithium 2,6-diformyl-4-methylphenolate (**3**), and unsymmetric lithium 2-acetyl-6-propanoyl-4-methyl phenolate (**4**) by variable temperature ^1H , ^7Li and/or ^{13}C NMR spectroscopy. Symmetric phenolates **2** and **3** behave identically as **1**, forming two tetrameric species **A** and **B** in CD_2Cl_2 with the **A/B** ratio higher in CDCl_3 or THF than in CD_2Cl_2 . Unsymmetric phenolate **4** forms at least five aggregates in CDCl_3 and CD_2Cl_2 . See the Supporting Information for details.

(11) The authors have deposited atomic coordinates, bond lengths and angles, and thermal parameters for structures **I**, **II**, and **V** with the Cambridge Crystallographic Data Centre (deposition number 100371). The data can be obtained, on request, from the Director, Cambridge Crystallographic Data Centre, 12 Union Road, Cambridge, CB2 1EZ, U.K.

(12) Another X-ray structure was obtained for phenolate **1** crystallized from THF by hexane diffusion at ambient temperature. The structure is also a tetramer of type **I**, but it has a monoclinic space group $P2_1/c$.

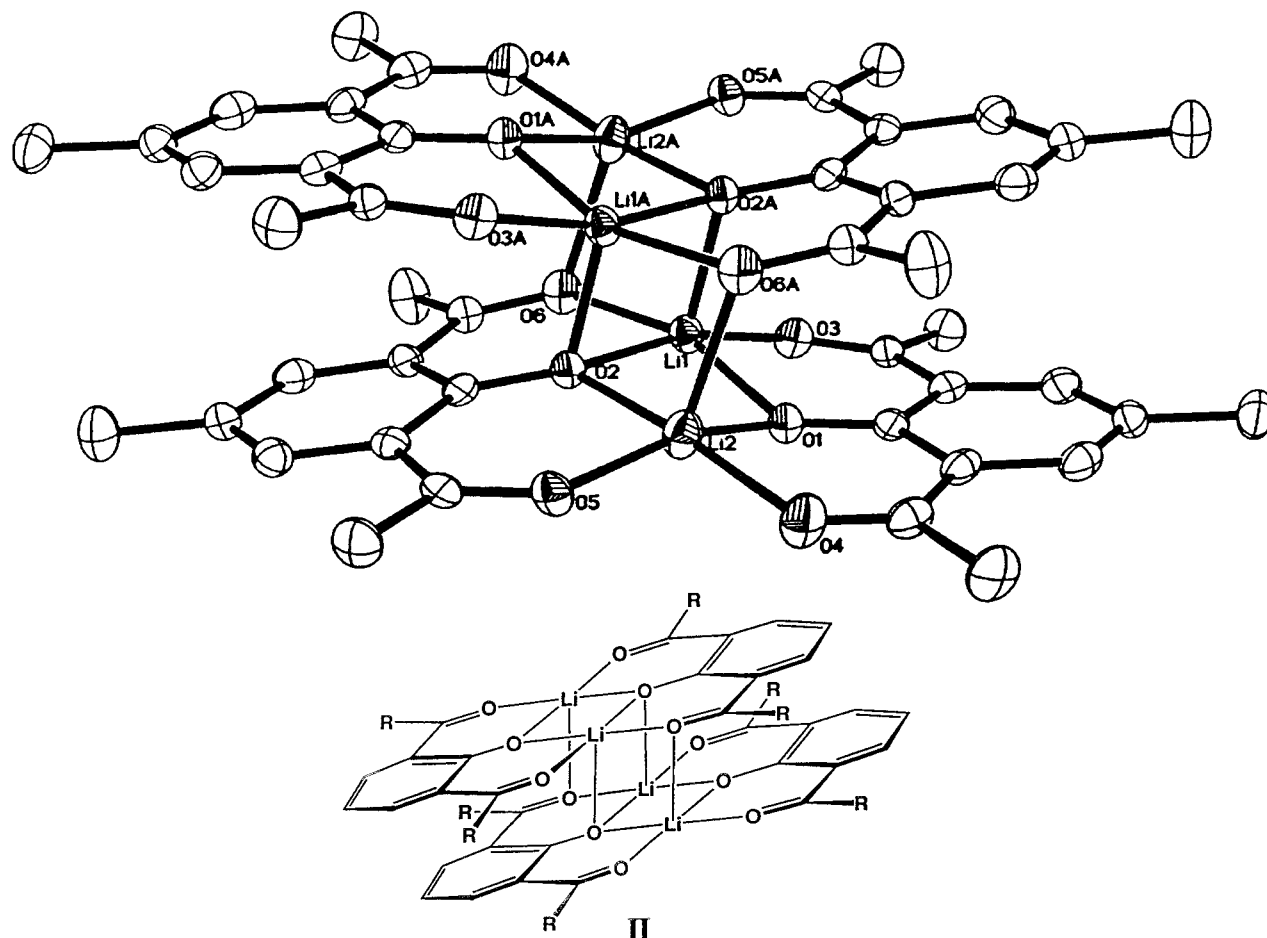


Figure 3. Molecular structure of diketone **II** (30% probability thermal ellipsoids). Important bond distances Li1–O2A 2.108 Å, Li2–O6A 2.355 Å, Li1–O3 1.991 Å, Li1–O1 1.961 Å, Li2–O1 1.938 Å, Li2–O4 1.955 Å.

Thus, the formation of one Li–O bond would be concerted with the breakage of another in a symmetrical transition state. In contrast, interconversion between tetramers **I** and **II** entails (a) breakage of three interdimer Li–O bonds; (b) rotation about the fourth interdimer Li–O bond; and (c) reformation of three interdimer bonds connecting each lithium with three oxygens which were originally 4.70, 3.65, and 3.65 Å away from the metal ions. Such an internal rotation has one or more non-symmetric transition states and requires more structural changes compared to a simple sliding motion and, thus, it should have a higher activation energy. This model would explain why rearrangement between **I** and **II** is much slower than a “sliding motion” in **II**.

An alternative possibility is that tetramer **III**, drawn below, represents **A** or **B** even though such a structure was not isolated in the solid state. As with tetramer **I**, tetramer **III** has equivalent aromatic rings, but (to its

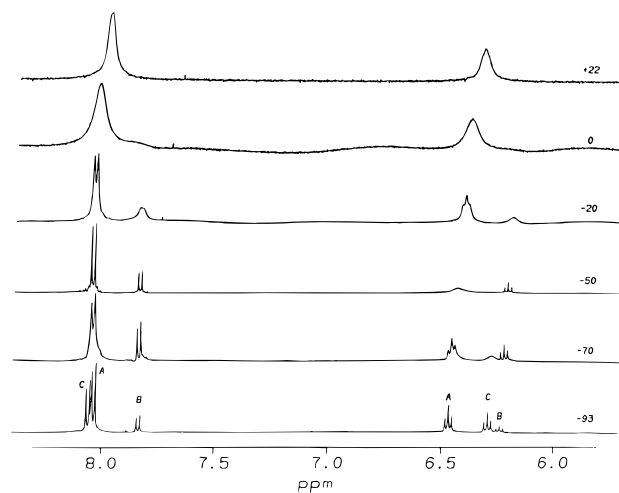
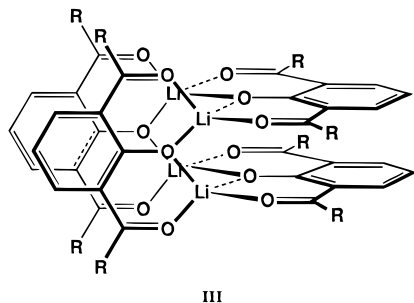


Figure 4. Selected variable temperature ^1H NMR spectra (aromatic region) for 0.028 M **I** in $\text{CD}_2\text{Cl}_2/\text{THF}$ 1:1 mixture.

discredit) it also positions the partially negative oxygens and partially positive carbons directly above one another.

The situation is more complicated for **1** in $\text{THF}-d_8$ and in $\text{CD}_2\text{Cl}_2/\text{THF}-d_8$ mixtures: a third component **C** appears. As seen in Figure 4, **C** has the same splitting patterns as **A** and **B**. Since at -50°C in Figure 4 the signals for **A** and **C** have coalesced, leaving **B** unperturbed, **A** clearly equilibrates much faster with **C** than does **B** with **C** or **A** with **B**. Concentration-dependence studies of phenolate **1** in $\text{THF}-d_8$ plus titration studies

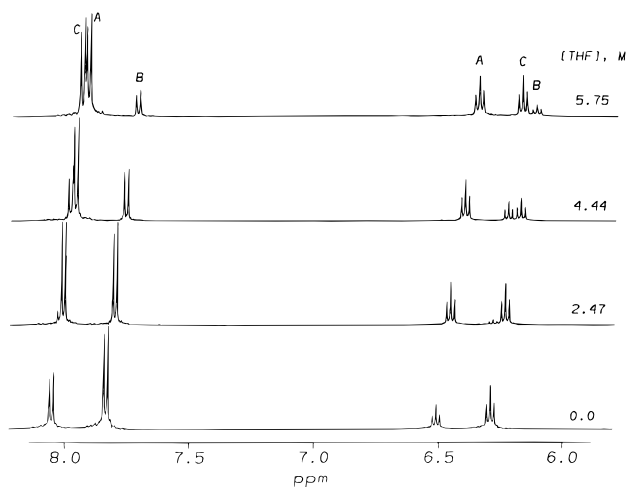
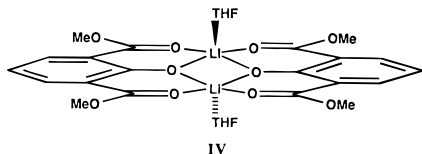
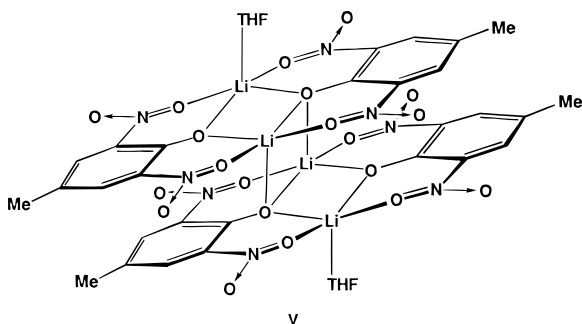


Figure 5. Selected ^1H NMR spectra (aromatic region) for THF- d_8 titration of 0.036 M **1** in CD_2Cl_2 .

of 0.036 M **1** in CD_2Cl_2 with THF- d_8 (Figure 5) are consistent with a model in which **A** (solvated by an average of 1.1–1.2 molecules of THF at 4:1 to 3:2 $\text{CD}_2\text{Cl}_2/\text{THF-}d_8$ ratio or by two THF molecules at higher dilutions with THF) breaks up into a dimer **C** that is solvated by two THF molecules. Since tetramer **B** remains unsolvated by THF, the **A:B** ratio increases upon addition of THF. A proposed structure (**IV**) for the THF-solvated dimer **C** is based on the recently elucidated crystal structure of lithium picrate monohydrate dimer^{3,8c} with C_{2h} symmetry: one water molecule, two phenolate oxygens, and two nitro oxygens coordinate to each lithium in a square pyramidal geometry.



THF-solvated **A** is thought to derive from tetramer-type **II** on the basis of our crystal structure of THF-solvated tetrameric lithium 2,6-dinitro-4-methylphenolate **V**. The compound resembles **II** except that both long $\text{Li}-\text{O}=\text{C}$ bonds (2.35 Å) have been broken by THF with inversion of lithium square pyramidal configuration. The $\text{Li}-\text{O}(\text{THF})$ bond in **V** is only 1.96 Å. By default one can postulate guardedly that **B** corresponds to structure **I**; solvation by THF does not occur owing, perhaps, to the shorter interdimer $\text{Li}-\text{O}$ bond.



Experimental Section

NMR Sample Preparation and Measurements. Solutions of lithium phenolates were prepared from corresponding phenols by reaction with an excess LiH at ambient temperature in

CDCl_3 , THF, or CD_2Cl_2 , and then filtered directly into an NMR tube via a plug of LiH under dry nitrogen. Solutions were stable for at least 1 week and can be quantitatively converted back to pure starting phenols by shaking with 2 M HCl. Molar concentration of phenolates were estimated from weights of starting phenols and solvents. ^1H and ^7Li NMR spectra were recorded on GN-500MHz spectrometer. Samples were equilibrated at each temperature for 5–10 min before recording the spectra. The probe was calibrated with standard MeOH sample, though reported temperatures are not corrected.

Selected NMR Data for Lithium Phenolates 1–3 (^1H NMR at 500 MHz, TMS = 0.000 ppm unless otherwise noted; ^7Li NMR at 184 MHz).

1: CD_2Cl_2 , ^1H NMR, +35 °C, δ 7.93 (broad d, $J_3 > 6.5$ Hz, 2H), 6.31 (broad t, $J_3 > 6.5$ Hz, 1H), 3.66 (s, 6 H); –85 °C, mixture of two isomers with integral ratio **A:B** = 36:64, δ 8.05 (d, $J_3 = 8.0$ Hz, 0.72 H, **A**), 7.83 (d, $J_3 = 8.0$ Hz, 1.28 H, **B**), 6.51 (t, $J_3 = 8.0$ Hz, 0.36H, **A**), 6.28 (t, $J_3 = 8.0$ Hz, 0.64 H, **B**), 3.68 (s, 3.84H, **B**), 3.63 (s, 2.16H, **A**); –30 °C, the same as at –85 °C but **A:B** = 43:57, coalescence temperature $T_c = +5$ °C for both *meta*- and *para*-ArH, $T_c = -5$ °C for Me. ^7Li NMR: rt, one broad singlet; low temperature, two singlets with the integral ratio in agreement with ratio in ^1H NMR.

2: CD_2Cl_2 , ^1H NMR, –85 °C, **A:B** = 96:4, δ 7.845 (s, 1.92H, **A**), 7.593 (s, 0.08H, **B**), 2.468 (s, 5.76H, **A**), 2.381 (s, 0.24H, **B**), 2.326 (s, 2.88H, **A**), 2.297 (s, 0.12H, **B**); –10 °C, **A:B** = 85:15; +35 °C, **A:B** = ca. 3:2, 7.7 (very broad s, 1.2 H, **A**), 7.5 (very broad s, 0.8H, **B**), 2.5 (very broad s, 6H); 2.33 (broad s, 3H). $T_c > 35$ °C for ArH, +30 °C for MeC(O)–, +20 °C for ArMe. ^7Li : low temperature, two broad signals with integral ratio in agreement with ^1H NMR.

3 (lithium 2,6-diformyl-4-methylphenolate): CD_2Cl_2 , –90 °C, **A:B** = 4:96, δ 9.483 (s, 0.08H), 9.163 (s, 1.92H), 7.612 (s, 0.08H), 7.270 (s, 1.92H), 2.366 (s, 0.12H), 2.325 (s, 2.88H). CDCl_3 , –60 °C, **A:B** = 63:37, δ 9.510 (s, $W_{1/2} = 2.67$ Hz, 1.25H), 9.186 (broad s, $W_{1/2} = 16.7$ Hz, 0.75H), 7.537 (s, $W_{1/2} = 2.74$ Hz, 1.25H), 7.209 (broad s, $W_{1/2} = 11.0$ Hz, 0.75H), 7.302 (CHCl_3 , $W_{1/2} = 0.80$ Hz), 2.317 (s, $W_{1/2} = 3.47$ Hz, 1.9H), 2.289 (broad s, $W_{1/2} = 7.87$ Hz, 1.1H); +10 °C, **A:B** = 31:69; $T_c = +30$ °C for CHO and ArH. ^7Li : two broad signals at low temperature with the same integral ratio as in ^1H NMR.

Concentration Dependence Studies and NMR Titration.

To find the aggregation number for **C**, three samples of **1** in THF was prepared to give **A:B:C** integral intensity ratios of 50:ca. 2:27 at 0.11 M, 23:ca. 1:23 at 0.057 M, and 20:ca. 1:51 at 0.021 M at –93 °C which correspond to tetramer–dimer equilibrium for **A** and **C**. For the titration, the 0.036 M solution of **1** in CD_2Cl_2 was gradually diluted with THF- d_8 and ^1H NMR spectra were taken at –93, –85, and –80 °C for a total of 10 dilutions. Concentration of **1** and its aggregates **A**, **B**, and **C** were calculated with the dilution correction from integral intensities for *para*-ArH proton. The differences between solvation numbers for **A**, **B**, and **C** can be found from corresponding equilibrium e.g. by plotting $\log([\text{A}]/[\text{B}])$ vs $\log([\text{THF}])$ for $\text{B} + n\text{THF} = (\text{A})(n\text{THF})$ equilibrium where n is the difference in solvation numbers for **A** and **B**. See Supporting Information for details.

Structure Determination.

Crystal data for **1**: rhombohedral pale yellow crystals, 0.20 × 0.24 × 0.36 mm, asymmetric unit $[\text{C}_{10}\text{H}_9\text{LiO}_5]_4$, $M = 864.45$, monoclinic space group $P2_1/n$ (No. 14); $a = 9.308(2)$, $b = 12.8830(10)$, and $c = 35.140(2)$ Å, $\beta = 94.220(10)^\circ$, $V = 4202.4(10)\text{Å}^3$, $Z = 4$, $\rho_{\text{calcd}} = 1.366\text{ g/cm}^3$, 7511 reflections were collected at 295 K with Cu K α ($\lambda = 1.54178$ Å) radiation on Siemens P4RA single crystal diffractometer with Cu rotating anode for $2.52^\circ < \theta < 56.73^\circ$. The structure was solved by direct methods (SHELXTL/PC v.5.03) and refined with full-matrix least squares on F^2 using 5443 unique intensity data to $R1 = 9.36\%$ ($wR2 = 0.2485$) after convergence for 578 parameters.

Crystal data for **2**: rhombohedral yellow crystals, 0.30 × 0.40 × 0.50 mm, $[\text{C}_{11}\text{H}_{11}\text{LiO}_3]_4$, $M = 792.55$, monoclinic space group $P2_1/c$ (No. 14), $a = 9.2593(10)$, $b = 14.569(2)$, and $c = 15.040(2)$ Å, $\beta = 100.488(9)^\circ$, $V = 1994.9(4)\text{Å}^3$, $Z = 2$ (asymmetric unit $[\text{C}_{11}\text{H}_{11}\text{LiO}_3]_2$), $\rho_{\text{calcd}} = 1.319\text{ g/cm}^3$, $\lambda = 1.54178$ Å, $T = 173$ K. A total of 3176 reflections were collected on Siemens P4RA diffractometer for $4.26^\circ < \theta < 56.74^\circ$. The structure was solved by direct methods, and all non-hydrogen atoms were anisotro-

pically refined by least squares to $R1 = 6.68\%$ ($wR2 = 0.2206$) after convergence for 2462 reflections and 272 parameters.

Crystal data for lithium 2,6-dinitro-4-methylphenolate $\cdot \frac{1}{2}$ THF: rhombohedral dichroic yellow/orange crystals, $0.26 \times 0.44 \times 0.48$ mm, $[\text{C}_7\text{H}_5\text{N}_2\text{O}_5\text{Li} \cdot (\text{C}_4\text{H}_8\text{O})_{1/2}]_4$, $M = 960.49$, triclinic space group $P\bar{1}$ (No. 2), $a = 8.4082(7)$, $b = 12.2106(11)$, and $c = 12.4769(13)$ Å, $\alpha = 117.721(7)^\circ$, $\beta = 99.278(8)^\circ$, $\gamma = 99.128(8)^\circ$, $V = 1078.4(2)$ Å³, $Z = 1$ (asymmetric unit $[\text{C}_{14}\text{H}_{10}\text{O}_{10}\text{N}_4 \cdot (\text{C}_4\text{H}_8\text{O})]$), $\rho_{\text{calcd}} = 1.479$ g/cm³, $\lambda = 0.71073$ Å, $T = 297$ K. A total of 3328 reflections were collected on Siemens P4 single-crystal diffractometer fitted with a Mo sealed tube X-ray source for $1.91^\circ < \theta < 22.50^\circ$. The structure was solved by direct methods, and all non-hydrogen atoms were refined by least squares against F^2 to $R1 = 5.43\%$ ($wR2 = 0.1669$) for 2663 reflections and 317 parameters.

Acknowledgment. This work was supported by the National Science Foundation. We are grateful to Prof. Karl Hagen for his guidance in X-ray structure elucidation. Special thanks goes to Prof. David Collum for invaluable discussions.

Supporting Information Available: X-ray data for structures **I**, **II**, and **V**, variable temperature NMR spectra for **1**, **2**, **3**, and **4**, and data for THF titration (30 pages). This material is contained in libraries on microfiche, immediately follows this article in the microfilm version of the journal, and can be ordered from the ACS; see any current masthead page for ordering information.

JO971102J